

# Swarm Intelligence Approach to 3D Medical Image Segmentation

Marta Galinska and Pawel Badura

**Abstract** In this paper we present a new idea for 3D medical image segmentation based on swarm intelligence and ant colony optimization. The methodology combines selected mechanisms running both mentioned artificial intelligence techniques, e.g. fitness-controlled motion of virtual agents or stigmergy. Foundations of the algorithm are described along with its implementation specification, simulations, results and their analysis also in terms of clarifying the parameterization. Several parameters are introduced and verified in terms of their influence on the method performance. The experiments rely on the segmentation of spleen in computed tomography studies. We also formulate some conclusions on possible ways for the algorithm future development.

**Keywords** Image segmentation · Swarm intelligence · Ant colony optimization

## 1 Introduction

Computer-aided diagnosis (CAD) systems designed e.g. for cancer diagnostics or post-treatment monitoring rely on proper analysis of medical images [7]. In most cases they require the expert contours of the region of interest (ROI) and/or the anatomical structure under consideration. The proper delineation and annotation stands for a diagnostic or pre-treatment factor of great importance. There is a large margin of error which depends on the expert when the structure contours are outlined manually [19]. They depend on the expert experience, age and even mood or time of the day. The intra-observer delineation may vary, since the results are considered unrepeatable and the segmentation gold standard is very difficult to detain. Moreover, the process of creating a contour is very laborious. All these factors force a

---

M. Galinska (✉) · P. Badura  
Faculty of Biomedical Engineering, Silesian University of Technology,  
Roosevelta 40, Zabrze, Poland  
e-mail: marta.galinska@polsl.pl

need to automate and objectify the segmentation process in diagnostic imaging. Making direct diagnostic decision based on automatic segmentation is, however, hardly acceptable. The semi-automatic methods are more appropriate: a person initiates, improves and controls the results of the algorithm (e.g. localizes the seed points or sets up parameters) but no delineations are made manually only.

Many standards for providing the partial automation of the image segmentation processes have been proposed through the years [9, 18]. None of them can be treated as a solution for all the problems, since each one addresses some specific issue. The topic of traditional 2D images segmentation have been explored particularly deeply, yet with a rapid progress in both, medical imaging data availability and computing power, the 3D processing techniques become more common nowadays. Such a growth of the amount of information brings also new challenges for intelligent analysis, requiring the employment of advanced processing and inference ideas. For that purpose, the artificial intelligence (AI) principles supply the segmentation workflows more often.

Artificial neural networks (ANN) and fuzzy logic (FL) are probably the most widely used AI branches in image segmentation in terms of ANN-based classification [21], fuzzy clustering [12, 25], fuzzy connectedness [5, 23], fuzzy inference systems [1] or hybrid neuro-fuzzy approaches [24]. The presence of evolutionary computation can also be noticed mostly in some specified auxiliary procedures like automated seed points selection [2, 14]. The granular computing have recently been employed for some pre-segmentation organ model definition [10]. The swarm intelligence ideas discovered actually in early 1990s are used in biomedical engineering mainly in bioinformatics [17, 20], yet also gradually appear in the image analysis domain. Multiple variants of the ant colony optimization (ACO) [8] and particle swarm optimization (PSO) [13] are, however, also mainly present as multipurpose procedures helpful at certain stages, not constituting the segmentation methodology itself. That concerns e.g. some sort of PSO-driven classifier training [26] or optimal multilevel threshold selection [15].

The ACO was initially illustrated by the traveling salesman problem [8]. Each virtual ant travels from one town to another and leaves pheromone on the road (stigmergy). The amount of pheromone depends on the road length. Pheromone evaporates over the time as it happens in nature [6]. The probability of choosing the next city on a track is directly proportional to the amount of pheromone on the path between the cities and inversely proportional to the distance among them [22]. The stigmergic information exchange makes the colony smart enough to search for the best solutions in a heuristic manner not only in the graph-defined approaches. The canonic ACO has been willingly modified. For example the ant colony behavior merged with beam search (which is a well-known tree search method) for open shop scheduling has been proposed [4]. The ACO hybridization with constraint programming (CP) and multilevel framework or auxiliary search space is also a well known technique [3].

PSO was designed to imitate social mechanisms observable in swarms or flocks consisting of more or less primitive individuals like birds, fish or insects [13]. Several basic rules control the swarm behavior [16], mainly related to collective searching

for a food and avoiding threats. The particle observes its neighbors, remembers its searching history and explores new spaces driven by some objective function. The PSO mathematical apparatus is very simple since it utilizes only basic arithmetic vector operations with a dose of randomness [13].

The goal of this study is to propose and examine a methodology based directly on swarm intelligence for segmentation of structures within medical imaging. We try to take advantage of possible correspondence of the 2D or 3D image space to the spatially-oriented PSO. The virtual agents exploring the image are stimulated by multiple factors, including the ACO-originating stigmergy. The paper describes implementation of the algorithm, experiments employing abdominal computed tomography (CT) studies, and analysis of the obtained results. Several parameters have been defined and analyzed for the swarm control with the awareness of the fact, that a lot of others are left for possible future formulation.

In the study we first introduce the virtual swarm specification in terms of its members, environment, parameters and auxiliary image processing techniques (Sect. 2). Then, the evaluation protocol is established in Sect. 3, followed by presentation and discussion on the obtained results. Conclusions are drawn in Sect. 4 along with a look at possible directions of the algorithm development.

## 2 Materials and Methods

The idea of the algorithm is to create a virtual swarm moving in a three-dimensional space related to the topology of the medical image. After the seed point location and parameters initialization, image preprocessing procedures are introduced (Fig. 1) in order to prepare the environment for the swarm operations. The iterative swarm motion is performed in the main loop in terms of the individuals particles movement.

### 2.1 PSO-Related Particle Movement Mechanisms

Each particle in the PSO algorithm has two main features in a  $D$ -dimensional problem space [13]: current position  $\mathbf{x} = \{x_i; i = 1 \dots D\}$  and current velocity  $\mathbf{v} = \{v_i; i = 1 \dots D\}$ , both initiated with random values. They are iteratively updated

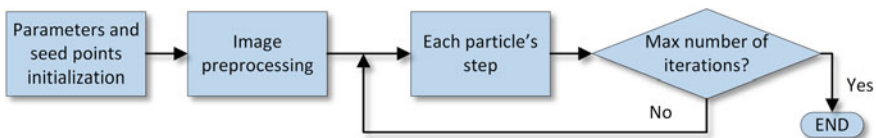


**Fig. 1** Block diagram of the algorithm

in accordance with:

$$v_i = wv_i + c_1r_1(\hat{x}_i - x_i) + c_2r_2(\hat{s} - x_i), \quad (1)$$

$$x_i = x_i + v_i, \quad (2)$$

where  $w$  is the inertia weight,  $r_1, r_2 \in [0, 1]$  are random variables,  $c_1, c_2$  are algorithm-specific constants,  $\hat{x}$  is the particle best location so far, and  $\hat{s}$  is the global best location reached by any particle within the swarm. The particles locations are evaluated using a fitness function  $f(\mathbf{x})$  subjected to optimization. Once the swarm moves throughout the environment, the communication mechanisms force the particles to search for optimal locations in an intelligent way.

Here, the particle is a sphere of a radius  $R$  temporarily centered in  $\mathbf{x}$  and moving with velocity  $\mathbf{v}$ .  $R$  is subjected to changes during the exploration with some limitations assumed for its value. The particles are placed in the environment—the image space—according to some predefined seed points, obtained in either, manual or automatic manner. During the exploration of the volume, particles leave certain amount of pheromone in visited places—indicate voxels that should belong to the resulting mask of the structure. In each iteration of the algorithm the attractiveness rate  $r$  for several selected voxels  $\mathbf{u}_j$  taken from the neighborhood  $\mathcal{N}(\mathbf{x})$  of the particle  $(\mathbf{x}, \mathbf{v})$  is calculated as:

$$r(\mathbf{u}_j) = a \cdot \frac{f}{\max(F)} + b \cdot \frac{f_d}{\max(F)} + c \cdot \frac{N_n}{N_a} + dm \cdot \frac{z}{||\mathbf{v}||}, \quad (3)$$

where:  $f$  denotes the amount of pheromone in  $\mathbf{u}_j$ ,  $f_d$ —the amount of pheromone on the path between  $\mathbf{x}$  and  $\mathbf{u}_j$ ,  $F$  is the matrix containing the distribution of pheromone in the image space,  $N_n, N_a$  are the numbers of neighbors and agents defined in the algorithm, respectively,  $z$  denotes the distance from the closest obstacle on the path (if present; obstacles are related to the image and  $m$  is a multiplier selected randomly from the set  $\{-1, 1\}$ ). The most attractive new location  $\hat{\mathbf{u}}$  for the agent is selected:

$$\hat{\mathbf{u}} = \arg \max_{j=1 \dots N_n} \{r(\mathbf{u}_j)\} \quad (4)$$

as it moves from  $\mathbf{x}$  to  $\hat{\mathbf{u}}$ .

The following main parameters have been introduced and tested:

**Number of agents**  $N_a$  defines the size of the swarm moving inside the mask. If the swarm is larger, we can expect the object to be segmented faster, yet the leak probability increases.

**Pheromone influence**  $a$  is one of the main parameters in assessing the attractiveness of the area. Its negative value discourages other particles from the already explored area and by this encourages them to explore new places.

**Pheromone evaporation**  $e$  during the exploration of the area particles leave pheromone in visited places. Each particle leaves the amount of pheromone equal

to  $(R - dist_p)$ , where  $dist_p$  denotes the distance between voxel  $p$  covered by the agent and its center  $x$ . The pheromone successively evaporates; its amount  $f$  is reduced at the end of each iteration:

$$f \leftarrow f - e. \quad (5)$$

**Search radius  $s$**  in millimeters determines the size of the area around the particle destination  $u_j$ , where all particles are recognized as neighbors. Large number of neighbors decreases the area attractiveness and probability of other particles displacement in this direction. A value of  $s$  should be moderate in order to affect the movement.

Additional parameters considered in the method include:

**The influence of pheromone on path  $b$**  Current direction of the particle is also influenced by the amount of pheromone on its way to the potential endpoint. This mechanism favors the previously unexplored paths.

**The influence of other particles  $c$**  The swarm intelligence idea offers some benefits of communication between the particles. Since we want to disperse the swarm to avoid duplication of visited area and expand the explored field, the stimuli should be negative.

**The influence of the path length  $d$**  The swarm has been divided into two parts:

- the part preferring long paths: particles specialized in fast, although imprecise exploration are responsible for the swarm movement and searching for new, large areas;
- the part preferring short paths: particles designed for local exploration are responsible for filling the mask and detecting contours.

**Size growth rate** The idea of the spherical particle volume increase—when it is in a *safe* place (away from the structure edge)—has a positive impact on the time of filling up the mask. The particle radius  $R$  is reduced upon collision in order to help the agent get through to less accessible spaces.

## 2.2 Image Data Influence on the Particle Movement

The image features: intensity and gradient have also an impact on the particles movement. Figure 2 shows a sample axial slice of the original abdominal CT study and its gradient. They determine restricted areas, which repulse the particle and make it rebound from the boundary of the structure. Two types of restrictions may apply here. On one hand, in case of binary features (e.g., a mask obtained at any pre-segmentation phase), a possible move from one point to another is restricted if an obstacle arises in-between. On the other hand, the real-valued features (intensity, gradient) can stimulate the agent in a fuzzy way, e.g., the closer to the image edge or surface indicated by a high gradient, the more intensive the repulsion affecting the particle. In this study we employed the binary restrictions. The original image data

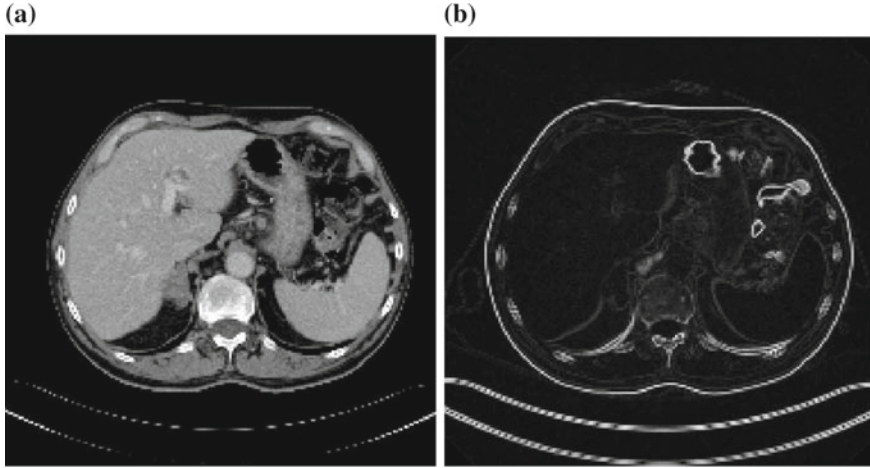


**Fig. 2** Sample original slice (a) and the gradient image (b)

have been initially thresholded in order to obtain the binary volume containing the spleen. The volume is then inverted, so the result indicates areas inaccessible for the particle. The second type of obstacles arise from the gradient image thresholding. Once the particle touches any obstacle, it immediately bounces back without leaving any pheromone.

### 3 Results and Discussion

The algorithm implemented in Matlab<sup>®</sup> has been tested using a database of five abdominal CT studies with spleen [11] delineated by an expert.<sup>1</sup> Intensity and gradient thresholds have been determined empirically for this kind of data at 60 Hounsfield units (HU) and 5.5 HU/mm, respectively. All volumes subjected to the analysis have been resampled in order to obtain a topology with a 2 mm linear voxel size in each direction. The results were conducted by repeating the algorithm with different sets of parameters. Each set was tested 5 times and the results were averaged to verify the repeatability. A total of 24 sets were tested (Table 1), yielding 120 runs per study. Seven seed points were selected manually and their location did not change throughout all runs. Two evaluation measures have been used—the sensitivity and Dice index:

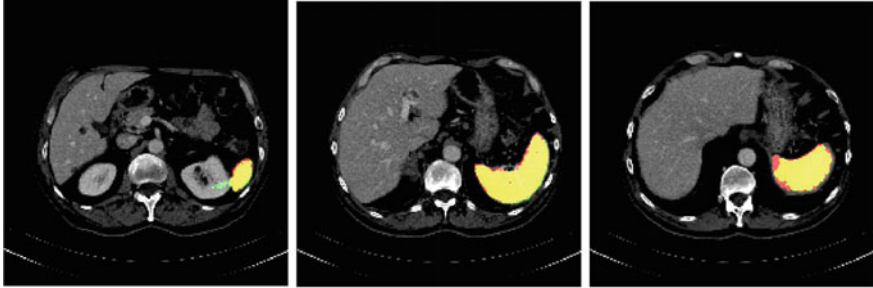
$$Sen = \frac{TP}{TP + FN} \cdot 100 \%, \quad (6)$$

---

<sup>1</sup>Diagnostic context plays only a supporting role to the main research on the swarm algorithm.

**Table 1** Summary of tested parameters

Parameter	$N_a$	$a$	$e$	$s$
Tested values	{300, 1500, 3000}	{-2, -1}	{0.00, 0.01}	{2, 5}

**Fig. 3** Illustration of a sample segmentation result. TP voxels in yellow, FN—red, FP—green. Swarm parameters:  $N_a = 3000$ ,  $a = -1$ ,  $e = 0$ ,  $s = 5$ 

$$D = \frac{2 \cdot TP}{2 \cdot TP + FP + FN} \cdot 100\%, \quad (7)$$

where  $TP$ ,  $FP$ ,  $FN$  denote the number of true positive, false positive, and false negative voxels, respectively (Fig. 3). Figure 4 shows the pheromone-marked voxels in subsequent iterations, whilst combined sensitivity and Dice index plots in time for different parameter sets are presented in Fig. 5. A great and consistent progress can be observed up to the ca. thirtieth iteration. Later iterations are responsible for the external object surface smoothing and possible leaks. Table 2 presents a summary of optimal parameter values based on the results analysis. As can be seen, the selection of parameters depends on the image. The only *universal* parameter is the number of particles, yet its value may depend on the segmented object size and character. Nonetheless, swarms with 3000 particles worked most efficiently. It is possible that a larger swarm would achieve better results yet, due to the computing time, increasing number of particles is not an optimal solution.

The doubled value of pheromone influence  $a$  has a positive impact on the result of segmentation, which forces the swarm members to communicate more extensively in three out of five cases. The difference in evaporation rate  $e$  does not significantly affect the algorithm sensitivity. However, in most cases, swarms achieve better results if the evaporation has taken place. This may be due to the fact that during first iterations there is a large randomness in the direction selection; thus, implementation of the evaporation mechanism allows for further correction of non-visited areas. Searching for other particles in some neighborhood also improves the algorithm performance. Selection of the appropriate search radius  $s$  depends on the image.

We have to take into account that both, ACO and PSO are heuristic methods, thus there is no guarantee for reaching the best solution. Such algorithms search for the optimal solution with a high level of randomness. The results are unique,

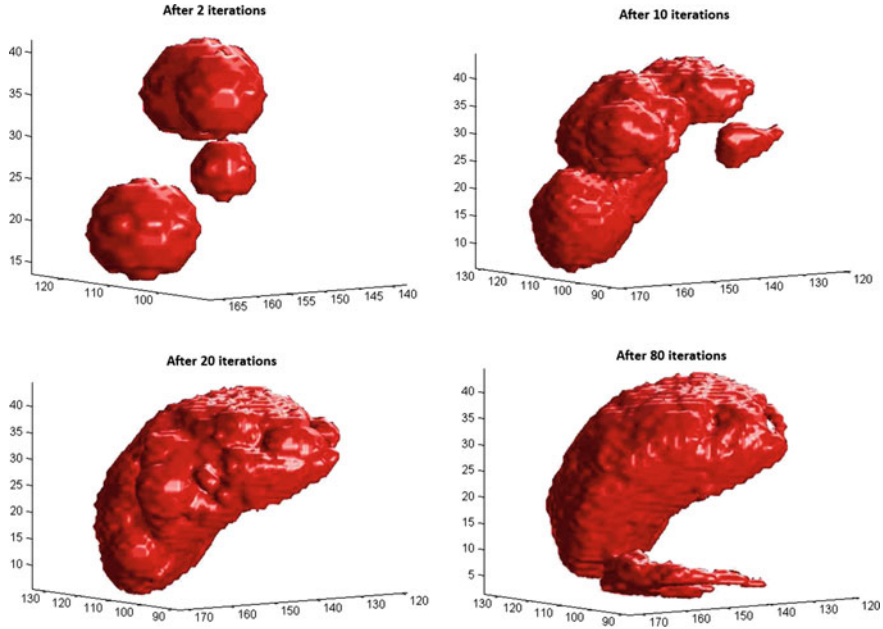


**Fig. 4** 3D visualization of the temporary segmentation result after 2, 10, 20 and 80 iterations. Obtained by the swarm with  $N_a = 3000$ ,  $a = -1$ ,  $e = 0$ ,  $s = 5$

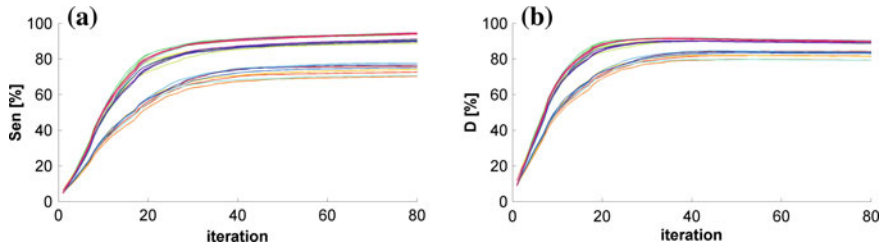


**Fig. 5** Combined sensitivity (a) and dice index (b) plots in time averaged throughout different parameter settings

therefore difficult in verifying. In this study such an unrepeatability has been treated with responsibility: the same sets of parameters have been applied five times. The randomness puts the method application in medicine into question, where repeatability of the results counts above everything else. Since our experiments employed a specific kind of segmentation problem, it is hard to formulate conclusive statements on generalized parameters settings. The development of a swarm intelligence-based approach to the image segmentation should therefore involve various types of imaging techniques and structures at the validation stage.

The use of the proposed solution is probably insufficient for diagnostic purposes in its current form, but it may be an auxiliary tool for the radiologist. It is also possible that the combination of the described method with other applicable AI or

**Table 2** Summary of the optimal parameter settings for individual studies

Image number	$N_a$	$a$	$e$	$s$	$Sen$ (%)	$D$ (%)
1	3000	−1	0	2	84	84
2	3000	−2	0.01	5	90	77
3	3000	−1	0	5	94	92
4	3000	−2	0.01	5	96	84
5	3000	−2	0.01	2	75	86

non-AI solutions would give satisfactory results. The method is very easy to modify because of its specificity. Adding new particle movement rules can improve the swarm efficiency. Going one step further we can risk hybridization of the method with evolutionary algorithms. This would reflect the natural Darwinism in the virtual population life, promoting more efficient individuals and removing the weak ones.

## 4 Conclusion

One of the purposes of this study was a verification if the particle motion randomness improves the efficiency of the performed task (in this case segmentation). The answer is not clear. Tracking the size and shape of segmented object shows that agents disperse from the seed points evenly. This allows for time saving in comparison to visiting all available voxels. There is a risk that at some stage the best direction could be skipped and a particle moves in another direction. Therefore, randomness might have a negative effect on the segmentation efficiency. However, the productivity of the algorithm in terms of time resources usually compensates this drawback, since the difference between the best of randomly drawn directions and the best of all available directions is usually very small. The main advantages of heuristic methods are the easily extensible number of criteria and the objective function adaptability. Although the current implementation operates directly in 3D medical image space which is not the most common case in this domain, one can imagine the swarm acting in a space of a higher dimensionality. That might concern images of different modalities, acquired during different examinations or employing various image features.

**Acknowledgments** This research was supported by the Polish National Science Center (NCN) grant No. UMO-2012/05/B/ST7/02136.

## References

1. Badura, P., Pietka, E.: 3D fuzzy liver tumor segmentation. *Inf. Technol. Biomed. Lect. Notes Bioinform.* **7339**, 47–57 (2012)
2. Badura, P., Pietka, E.: Semi-automatic seed points selection in fuzzy connectedness approach to image segmentation. *Comput. Recogn. Syst. Adv. Intell. Soft Comput.* **45**(2), 679–686 (2007)

3. Blum, C.: Ant colony optimization: introduction and recent trends. *Phys. Life Rev.* **2**(4), 353–373 (2005)
4. Blum, C.: Beam-ACO-hybridizing ant colony optimization with beam search: an application to open shop scheduling. *Comput. Oper. Res.* **32**, 1565–1591 (2005)
5. Czajkowska, J., Badura, P., Pietka, E.: 4D segmentation of Ewing's sarcoma in MR images. *Inf. Technol. Biomed. Adv. Intell. Soft Comput.* **69**(2), 91–101 (2010)
6. Deneubourg, J., Pasteels, J., Verhaeghe, J.: Probabilistic behavior in ants—a strategy of errors. *J. Theor. Biol.* **105**(2), 259–271 (1983)
7. Doi, K.: Computer-aided diagnosis in medical imaging: historical review, current status and future potential. *Comput. Med. Imaging Graph.* **31**(4–5), 198–211 (2007)
8. Dorigo, M., Maniezzo, V., Colomi, A.: Ant system: optimization by a colony of cooperating agents. *IEEE Trans. Syst. Man Cybern. Part B* **26**(1), 29–41 (1996)
9. Gonzalez, R., Woods, R.: *Digital Image Processing*. Prentice Hall (2008)
10. Juszczuk, J., Pietka, E., Pycinski, B.: Granular computing in model based abdominal organs detection. *Comput. Med. Imaging Graph.* **46**(2), 121–130 (2015)
11. Kawa, J., Juszczuk, J., Pycinski, B., Badura, P., Pietka, E.: Radiological atlas for patient specific model generation. *Inf. Technol. Biomed. Adv. Intell. Syst. Comput.* **284**(4), 69–82 (2014)
12. Kawa, J., Pietka, E.: Image clustering with median and myriad spatial constraint enhanced FCM. *Comput. Recogn. Syst. Adv. Intell. Soft Comput.* **45**, 211–218 (2005)
13. Kennedy, J., Eberhart, R.C.: Particle swarm optimization. In: *Proceedings. IEEE International Conference on Neural Networks*, pp. 1942–1948 (1995)
14. Liang, Y., Zhang, M., Browne, W.: Image segmentation: a survey of methods based on evolutionary computation. In: *Simulated Evolution and Learning, Lecture Notes in Computer Science*, vol. 8886, pp. 847–859 (2014)
15. Maitra, M., Chatterjee, A.: A hybrid cooperative-comprehensive learning based PSO algorithm for image segmentation using multilevel thresholding. *Expert Syst. Appl.* **34**(2), 1341–1350 (2008)
16. Millonas, M.M.: *Swarms, phase transitions, and collective intelligence*. In: *Artificial Life III*. Addison-Wesley (1994)
17. Mohamad, M.S.: An enhancement of binary particle swarm optimization for gene selection in classifying cancer classes. *Algorithm Mol. Biol.* **8**(1), 1–11 (2013)
18. Pham, D., Xu, C., Prince, J.: Current methods in medical image segmentation. *Ann. Rev. Biomed. Eng.* **2**, 315–337 (2000)
19. Pietka, E., Kawa, J., Spinczyk, D., Badura, P., Wieclawek, W., Czajkowska, J., Rudzki, M.: Role of radiologists in CAD life-cycle. *Eur. J. Radiol.* **78**(2), 225–233 (2011)
20. Roseffeld, S.: Critical junction: nonlinear dynamics, swarm intelligence and cancer research. In: *IEEE Symposium on Computational Intelligence in Bioinformatics and Computational Biology*, pp. 206–211 (2013)
21. Sharma, N., Ray, A., Sharma, S., Shukla, K., Pradhan, S., Aggarwal, L.: Segmentation and classification of medical images using texture-primitive features: application of BAM-type artificial neural network. *J. Med. Phys.* **33**(3), 119–126 (2008)
22. Simon, D.: *Evolutionary Optimization Algorithms*. John Wiley and Sons (2013)
23. Udupa, J., Samarasekera, S.: Fuzzy connectedness and object definition: theory, algorithms, and applications in image segmentation. *Graph. Model Image Process.* **58**(3), 246–261 (1996)
24. Verma, B., Zakos, J.: A computer-aided diagnosis system for digital mammograms based on fuzzy-neural and feature extraction techniques. *IEEE Trans. Inf. Technol. B* **5**(1), 46–54 (2001)
25. Zarychta, P.: Features extraction in anterior and posterior cruciate ligaments analysis. *Comput. Med. Imaging Graph.* **46**(2), 108–120 (2015)
26. Zyout, I., Czajkowska, J., Grzegorzec, M.: Multi-scale textural feature extraction and particle swarm optimization based model selection for false positive reduction in mammography. *Comput. Med. Imaging Graph.* **46**(2), 95–107 (2015)

Information Technologies in Medicine

5th International Conference, ITIB 2016 Kamień Śląski,

Poland, June 20 - 22, 2016 Proceedings, Volume 1

Piętka, E.; Badura, P.; Kawa, J.; Wieclawek, W. (Eds.)

2016, XII, 518 p. 262 illus., 124 illus. in color., Softcover

ISBN: 978-3-319-39795-5